

Modelling of vertical-cavity surface-emitting laser beam collimation using a nanostructured gradient index microlens

JĘDRZEJ M. NOWOSIELSKI^{1,2}, ANDREW J. WADDIE¹,
MOHAMMAD R. TAGHIZADEH¹, RYSZARD BUCZYŃSKI^{1, 2*}

¹Heriot-Watt University, School of Engineering and Physical Sciences,
Edinburgh EH14 4AS, Scotland, UK

²University of Warsaw, Faculty of Physics,
Pasteura 7, 02-093 Warsaw, Poland

*Corresponding author: ryszard.buczynski@itme.edu.pl

In this paper we show that the recently developed nanostructured gradient index (nGRIN) rod microlens can be utilised for the collimation of the beam generated by a vertical-cavity surface-emitting laser (VCSEL). The modelling of the nanostructured lens structure is performed using the finite difference time domain (FDTD) method with realistic nGRIN parameters and a Gaussian model of the light source. The large refractive index gradient of the nanostructured microlens allows the final microlens thickness to be only 70 μm with a diameter of 10 μm . Successful collimation of a single-mode VCSEL beam with a waist half-width of 1.53 μm is presented with a reduction in divergence half-angle from 10.1° to 3.3° . We show that the linear polarisation of the incident beam is preserved as well as presenting the tolerance of this type of lens to variations in overall thickness.

Keywords: gradient index optics, microlens, soft glass.

1. Introduction

Gradient index (GRIN) optical elements are particularly suitable for laser beam shaping in practical systems due to their flat input and output facets which facilitate their integration with other optoelectronic components [1, 2]. Vertical-cavity surface-emitting lasers (VCSELs), which generally generate high divergence single-mode Gaussian beam profiles, can be fabricated in high density 2D arrays [3]. The combination of a GRIN microlens array and an identical pitch VCSEL array would allow the creation of low divergence structured light sources for optical interconnects, printers and scanners [4].

The recent introduction of the nanostructured gradient index (nGRIN) rod microlens, which consists of assemblies of parallel subwavelength diameter glass rods allows the fabrication of microlens arrays precisely matched to the emission characteristics of the micro-lasers under consideration [5–7]. The nGRIN microlenses are fabricated using the modified stack and draw technique widely used in the production of photonic crystal fibres [8]. This technique enables the fabrication of microlenses characterised by very high refractive index gradients (up to $\Delta n = 0.1$ per $5 \mu\text{m}$) and high numerical aperture. Moreover the microlenses can be monolithically arranged into 2D arrays, exploiting the same fabrication process, with a filling factor close to 100%. The nanostructured GRIN microlens arrays are very thin (about $100 \mu\text{m}$ thick) with flat input and output facets simplifying their integration with a high density 2D VCSEL array in order to collimate the beams generated by the VCSELs. The concept of the system is shown in Fig. 1 and in this paper we present FDTD simulation results for a single microlens integrated with a VCSEL laser.

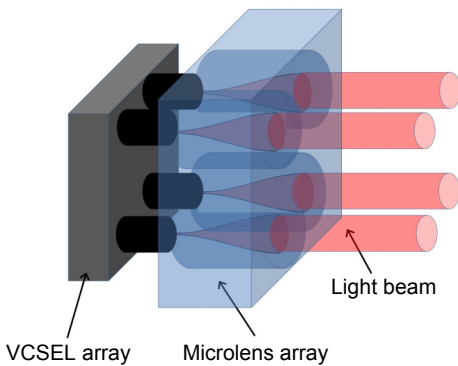


Fig. 1. Collimation of a VCSEL array by means of an array of flat-facet nGRIN microlenses.

We have shown that the Gaussian beam formalism can be successfully applied to describe beam propagation in a nanostructured gradient index medium [7]. In this paper we show results of modelling devoted to a particular application of nGRIN lens for the collimation of VCSEL lasers. Collimation of large 2D arrays of vertical-emitting sources is an important issue and current solutions suffer from high complexity of the optical and packaging systems.

In this paper we consider a small microlens diameter of $10 \mu\text{m}$ with a view to obtaining a collimated beam with a relatively small beam diameter, suitable for addressing ultra-densely packed arrays of optoelectronic components for free-space optical interconnects. Currently the standard pitch of VCSEL is $200\text{--}250 \mu\text{m}$ and several types of collimation microlens arrays have been proposed and successfully implemented [9]. However if further miniaturization of optoelectronic systems is required, a more dense array of microlenses will be necessary. In particular, the inter-

connection of integrated optical circuits and external arrays of sources, detectors or multicore fibers is an open issue [10]. In this case, the development of highly efficient microlenses using the standard refractive or diffractive approaches is an unresolved technological challenge.

2. Design and development of the nGRIN microlenses

The performance of nGRIN microlenses, which consist of a few thousand subwavelength nanorods arranged parallel to each other, is based on the effective medium theory [11]. Each nanostructured lens is composed of two types of nanorod characterised by different refractive indices and similar mechanical and thermal properties. The cross-section of the nanostructured microlens investigated in this paper is presented in Fig. 2.

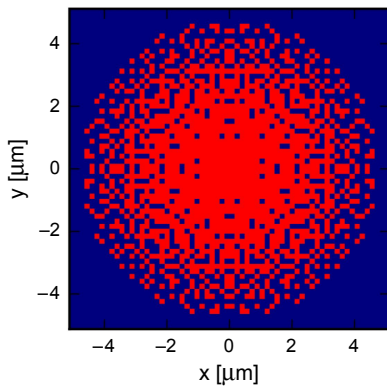


Fig. 2. The refractive index distribution in the cross-section of the nGRIN microlens. Every pixel represents a single subwavelength rod with typical square cross-section of $160\text{ nm}\times 160\text{ nm}$. Colours represent two types of rods made of two types of glass vary in refractive index ($n_1 = 1.6190$ and $n_2 = 1.6088$). Distribution of rods determines performance of the lens.

The individual glass rods in the microlenses have diameters much less than the wavelength of the incident light (typically $100\text{--}200\text{ nm}$) and can therefore be described by an averaged refractive index distribution using an effective medium theory. In order to obtain the effective refractive index at a given point within the microlens, assuming no absorption by the constituent glasses, one simply calculates a volume average of the permittivity within the immediate neighbourhood of that point. The diameter of this neighbourhood is typically around one wavelength and the experimental and modelling results presented in [5–7] show that this approximation is valid for the nanorod diameters under consideration here. This approach was inspired by the Maxwell–Garnet mixing formula [11], which defines the effective permittivity ϵ_{eff} of a structured medium where homogeneous spherical dielectric inclusions are ran-

domly distributed in a homogeneous dielectric host medium. The Maxwell–Garnet mixing formula is usually presented as [11]

$$\varepsilon_{\text{eff}} = \varepsilon_e + 3f\varepsilon_e \frac{\varepsilon_i - \varepsilon_e}{\varepsilon_i + 2\varepsilon_e - f(\varepsilon_i - \varepsilon_e)} \quad (1)$$

where f , ε_i and ε_e are the volume filling factor of inclusions, the permittivity of inclusions and the permittivity of host medium, respectively. When both permittivities are similar to each other one can use an approximation given by the first order Taylor expansion of formula (1)

$$\varepsilon_{\text{eff}} \approx \varepsilon_e + f(\varepsilon_i - \varepsilon_e) \quad (2)$$

which means that effective permittivity ε_{eff} is approximated by the volume average of the permittivity.

The design cycle of an nGRIN microlens begins by determining the ideal refractive index distribution required to produce the needed optical functionality. This ideal distribution is used as the reference within a simulated annealing optimisation algorithm where the effective medium approach is used to determine the averaged refractive index distribution given by discrete 2D nanorod distribution [12]. The refractive indices of the constituent glasses, the number of nanorods in the structure and their distribution are used as parameters in the optimisation algorithm. Finally the overall performance of the nanostructured lens is verified using a fully vectorial electromagnetic simulation algorithm such as the finite difference time domain (FDTD) method.

The nGRIN microlens array fabrication process, which exploits the well-known stack-and-draw method [8], is comprised of the following steps [5]. Firstly two types of glass, characterised by different refractive indices and similar mechanical and thermal properties, are cast as long rectangular bars which are then cut, ground and polished to obtain rods with a round or rectangular cross-section. These rods are then

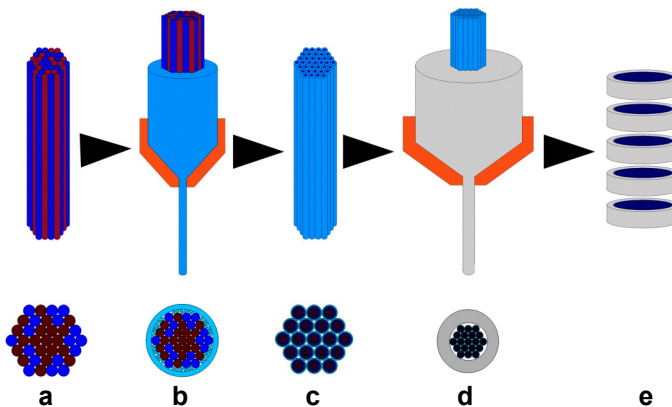


Fig. 3. Schematic of the fabrication procedure (see text for explanation).

scaled down, using a fibre drawing tower, to a diameter of 0.6–1 mm. Several hundreds of these rods are then stacked into an initial preform according to the designed rod distribution (Fig. 3a) and this is drawn-down at a low temperature in close proximity to the softening point of the selected glasses (usually in the range of 600–900 °C) (Fig. 3b). The drawn-down structured rods obtained from this stage are cut and re-stacked into an intermediate preform (Fig. 3c) which is drawn-down again (Fig. 3d). The re-stacking and draw-down stages presented in Fig. 3c can be repeated multiple times until the desired final nanorod diameter is achieved. Usually each draw-down stage scales the cross-section diameter of the structure down by a factor of 10–30. Finally, once the individual nanorod diameter is in the 100–200 nm range, the fabricated nanostructured rod is cut into slices, typically about 100 µm thick, each of which contains an identical array of nGRIN microlenses. It should be noted that it is possible to fabricate both rectangular- and hexagonal-packed arrays of microlenses by a suitable choice of rod cross-sectional shape during the initial preform assembly.

3. FDTD simulation of the VCSEL beam collimation

The goal of the finite difference time domain (FDTD) simulations is to verify performance of the designed nGRIN rod microlens and show their ability to collimate a VCSEL beam [13]. The freeware MEEP package was used in our case for simulations [14]. A single-mode VCSEL beam is approximated by a planar Gaussian beam described by the complex amplitude:

$$\psi(x, y, z = 0) = A \exp\left(-\frac{x^2 + y^2}{w_0^2}\right) \quad (3)$$

where w_0 is the half-width of the beam used in this paper. The VCSEL is assumed to emit a monochromatic beam at a wavelength of 850 nm with a beam half-width of $w_0 = 1.53 \mu\text{m}$. Assuming single-mode performance of the source ($M^2 = 1$), its numerical aperture is equal to $\text{NA} = 0.177$. The above-mentioned parameters of the source correspond to the VCSEL presented by SERKLAND *et al.* [15]. The spatial step of the FDTD simulation is equal to 25 nm and the time step is set to ensure numerical stability [14]. The perfectly matched layers (PML) absorbing boundary conditions are implemented to ensure no parasitic reflection in the simulation. To achieve collimation of such a beam, we consider a lens with a diameter of 10.24 µm. In this case, an effective focal length of about 28 µm is required in order to obtain a quarter pitch GRIN lens with similar numerical aperture as the VCSEL emitted Gaussian beam. In this case, the refractive index at the centre of the microlens cross-section is assumed $n_0 = 1.619$ and the gradient parameter is $g_0 = 22 \text{ mm}^{-1}$. The numerical aperture of the considered GRIN lens related to the maximum acceptance angle is $\text{NA} = 0.182$, higher than numerical aperture of an input beam. Therefore most of the energy will be transferred through the lens, however some minor diffraction effects can occur.

The effective refractive index distribution of the GRIN lens is given by:

$$n(x, y) = n_0 \left[1 - \frac{g_0^2}{2} (x^2 + y^2) \right] \tag{4}$$

where n_0 denotes the refractive index at the centre of the microlens cross-section and g_0 denotes the gradient parameter. The microlens consists of multiple glass rods of two types with refractive indices of 1.6190 and 1.6088. Each individual glass rod has a square cross-section and similar size of $0.16 \mu\text{m} \times 0.16 \mu\text{m}$. The lens is composed of an array of 64×64 rods (4096 rods in total). The total microlens diameter is $10.24 \mu\text{m}$. The refractive index distribution is calculated with the simulated annealing optimisation algorithm described in details in [5]. The cross-section of the optimised nGRIN microlens is shown in Fig. 2.

The calculated nGRIN structure is transferred into FDTD software as a 3D array. A schematic of the FDTD simulation of the VCSEL beam collimation is presented in Fig. 4. The VCSEL source and the input facet of the nGRIN microlens are located in the plane $Z_0 = 0$. According to the paraxial approximation, the quarter pitch lens, which has a length of $L_q = \pi/(2g_0)$, is optimal for VCSEL beam collimation [1]. In the case of the simulated nGRIN lens we expect the quarter pitch to be around $L_q = 71.4 \mu\text{m}$. The output plane Z_q in the following simulations is located at the distance $Z_q = Z_0 + L_q$ corresponding to the quarter pitch length of the GRIN lens.

The FDTD simulation is carried out at the distance of $80 \mu\text{m}$ and we have assumed that the infinite length of the nGRIN structure fills to ensure a proper identification of quarter pitch distance. The transversal size of the simulation area is $20 \mu\text{m} \times 20 \mu\text{m}$ with an overall nGRIN lens diameter of $10.24 \mu\text{m}$. The remaining area is filled with the low refractive index material ($n = 1.6088$), which represents a pad area of glass in the array. This approach is commonly used in simulation in the FDTD method to avoid numerical artefacts related to the proximity of the simulated structure to the PML area [13]. The intensity distribution along the propagation direction is presented in Fig. 5. Simulation shows that the beam is collimated. However only a full

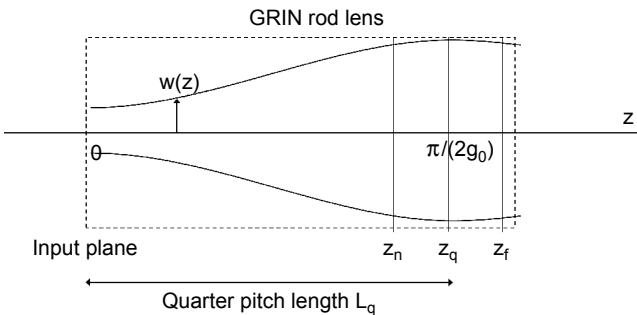


Fig. 4. Schematic of the FDTD simulation of the VCSEL beam collimation.

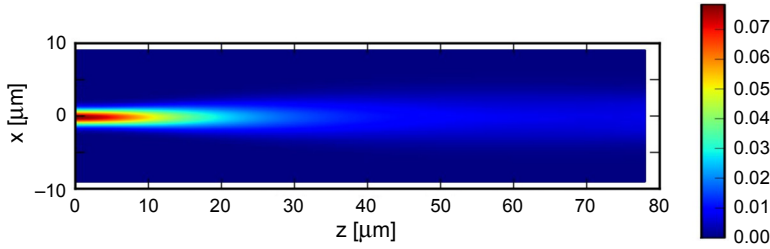


Fig. 5. The intensity distribution in the longitudinal cross-section of the FDTD simulation area. The z component of the time averaged Poynting vector is shown.

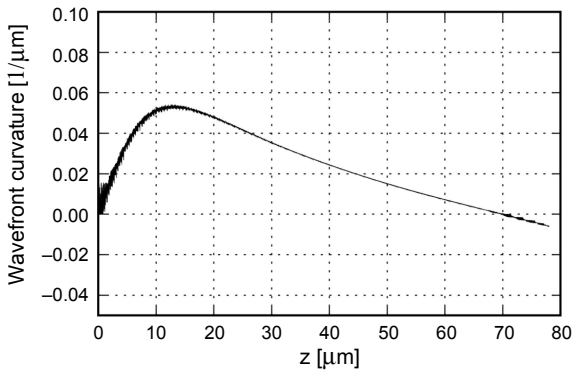


Fig. 6. Wavefront curvature as a function of the propagation distance.

wavefront analysis allows the precise determination of the quarter pitch of the GRIN lens [1].

A plot of the wavefront curvature as a function of the propagation distance is shown in Fig. 6. One can see that the wavefront is flat (with a curvature of zero) for a propagation distance of $z = 70 \mu\text{m}$. According to the analytic solution for the parabolic GRIN lens, the quarter pitch plane Z_q is located at the distance where the wavefront is flat [1]. Therefore for the considered nGRIN lens the quarter pitch length is $Z_q = 70 \mu\text{m}$. This value is very close to the theoretical value of quarter pitch length given by analytic solution $L_q = \pi/(2g_0) = 71.8 \mu\text{m}$. The difference between theoretical value and results of modelling is related to the fact that paraxial approximation is not fully valid in the case of the considered nGRIN lens since the gradient parameter g_0 is very high. The validity of the analytic solution in the case of nGRIN lenses is analysed in detail in [7].

The intensity distributions in the input plane Z_0 (VCSEL input plane) and the output plane Z_q (the quarter pitch distance) are shown in Fig. 7. The intensity profile obtained in the output plane Z_q is similar to a Gaussian profile (Fig. 8) and can be approximated with M^2 parameter equal to 1. Based on this result we can conclude that nanostructured

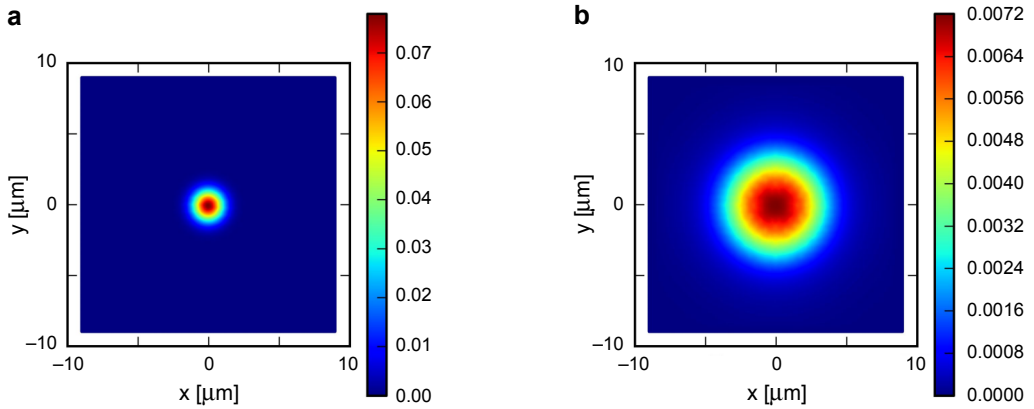


Fig. 7. The intensity distribution in the input plane $Z_0 = 0$ (a) and output plane Z_q at the distance of the quarter pitch (b). The z component of the time averaged Poynting vector is shown.

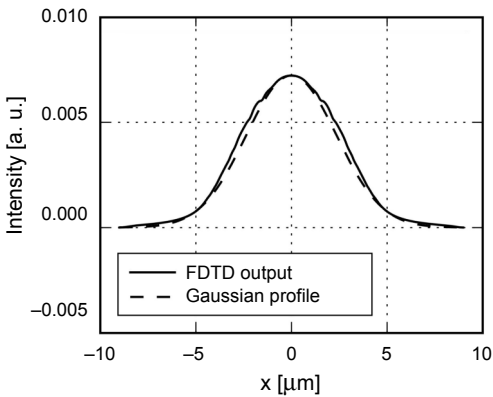


Fig. 8. The intensity profile in the output plane Z_q (solid line – FDTD output; dashed line – Gaussian beam fit with $M^2 = 1$ to FDTD output).

GRIN lens does not introduce any distortion into the beam propagation and the nGRIN lens performance is similar to an ideal GRIN lens.

At the output plane Z_q , the beam half-width is $w_{0q} = 4.7 \mu\text{m}$ and the wavefront is completely flat. In order to calculate the far field divergence half-angle θ , one can use

$$\theta = \frac{\lambda_0}{\pi w_0} \quad (5)$$

where θ denotes the divergence half-angle and $\lambda_0 = 850 \text{ nm}$ is the vacuum wavelength. The results of the FDTD simulations show a reduction in the VCSEL far field divergence half-angle from 10.1° to 3.3° due to the presence of the nGRIN microlens.

4. Analysis of polarisation properties of nGRIN

In general, it has been observed that the behaviour of the nanostructured material has a strong dependence on the polarisation of the incident light. This implies that the nGRIN lens performance might be affected by the input polarisation and, in consequence, the input polarisation state can be disturbed. We have analysed the FDTD simulations of the nGRIN microlens to verify the polarisation properties of the designed nGRIN lens. In the simulations, the incident beam of the VCSEL source has a linear polarisation (E_y) at the Z_0 plane. We have analysed the electric field components E_x and E_y of the beam in the output plane Z_q to determine the polarisation of the output beam (Fig. 9). The amplitude of the electric field components E_x is close to zero, while

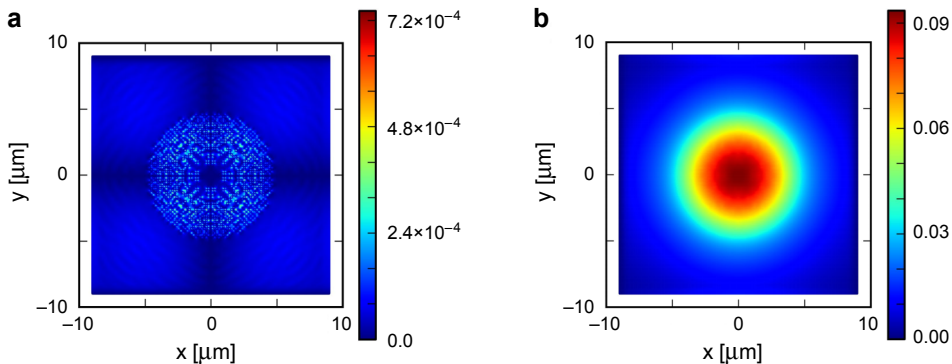


Fig. 9. Amplitudes of the electric field components in the output plane Z_q : component E_x (a) and component E_y (b).

the amplitude of the electric field components E_y is high. Therefore we can conclude that polarisation of the beam propagating through nGRIN is maintained. This behaviour can be easily explained by the irregular and deeply subwavelength structure of the lens. The distribution of both types of rods does not create any regular pattern that might create a subwavelength grating and the individual single rods are far too small to diffuse the light.

5. Tolerance analysis of the microlens length

The smallest divergence of the output beam is obtained when a quarter pitch microlens is utilised, which for the lens design presented in this paper corresponds to a nGRIN lens length of $L_q = 70 \mu\text{m}$. In practice, the microlens polishing process has a limited accuracy. Therefore a change of the nGRIN lens performance for its various lengths is important. The change in the beam divergence for a lens length error of $\pm 10\%$ shorter can be determined by calculating the wavefront curvature and the beam half-

-width in the proximity planes Z_n and Z_f (Fig. 4). The first proximity plane Z_n corresponds to a microlens length of $L_n = 63 \mu\text{m}$ and the second proximity plane Z_f corresponds to a microlens length of $L_f = 77 \mu\text{m}$.

The beam in the proximity plane Z_n , corresponding to a shorter nGRIN lens, can be approximated by a Gaussian beam with a wavefront curvature of $1/R_x = 0.0050 \mu\text{m}^{-1}$ based on Fig. 6 and beam half-width of $w_n = 4.7 \mu\text{m}$. Propagating this Gaussian beam in air allows the calculation of the beam waist w_{0n} and, hence, the far-field divergence half angle θ_n

$$\theta_n = \frac{\lambda_0}{\pi w_{0n}} \quad (6)$$

Assuming propagation in air, the inverse of the complex radius of curvature q_n is given by [16]

$$\frac{1}{q_n} = \frac{1}{R_n} - i \frac{\lambda_0}{\pi w_n^2} \quad (7)$$

and the variation of the complex radius $q(z)$ is given by the simple formula

$$q(z) = q_n + z - z_n \quad (8)$$

and therefore the imaginary part of $q(z)$ is constant. Moreover the complex radius q_{0n} for the beam waist is purely imaginary and can be written as

$$q_{0n} = i\Im\{q_n\} \quad (9)$$

where $\Im\{q_n\}$ denotes the imaginary part of q_n . On the other hand,

$$\frac{1}{q_{0n}} = -i \frac{\lambda_0}{\pi w_{0n}^2} \quad (10)$$

where w_{0n} is the waist half-width of the Gaussian beam. Using Eqs. (9) and (10), we obtain

$$\frac{-i}{\Im\{q_n\}} = -i \frac{\lambda_0}{\pi w_{0n}^2} \quad (11)$$

and hence

$$w_{0n}^2 = \frac{\lambda_0 \Im\{q_n\}}{\pi} \quad (12)$$

For the shorter lens length, this gives a waist half-width of $w_{0n} = 4.36 \mu\text{m}$ and from Eq. (6) a far field divergence half-angle of $\theta_n = 3.6^\circ$. The same derivation can be applied to the longer microlens, giving a beam waist half-width of $w_{0n} = 4.29 \mu\text{m}$ and

a far field divergence half-angle of $\theta_f = 3.6^\circ$. Based on calculation we can conclude that variation of the lens length by $\pm 10\%$ with respect to quarter pitch does not significantly influence the lens performance. In the studied cases the far field divergence half-angle increases by 0.3° up to 3.6° while the beam waist at the lens end facet is decreased from $4.7 \mu\text{m}$ to $4.29 \mu\text{m}$.

6. Conclusions

Simulations of a nanostructured GRIN microlens to collimate a single-mode VCSEL were presented in this paper. We have shown that using an nGRIN lens with a diameter of $10 \mu\text{m}$ and a length of $71 \mu\text{m}$, a reduction of the divergence half-angle from 10.1° to 3.3° can be achieved while maintaining a beam profile similar to the incident Gaussian profile without any distortion. Moreover the nGRIN microlens preserves the linear polarisation state of the incident beam. In addition, the microlens demonstrates a good tolerance to inaccuracies in the microlens length. If the microlens is 10% shorter or longer than the exact quarter pitch length, the divergence half-angle is increased to 3.6° . The stack-and-draw nanostructuring technology enables us to fabricate arrays of such nanostructured microlenses with almost 100% fill factor and therefore the presented simulation shows that a nanostructured microlens array can be utilized for collimation of a highly density packed 2D VCSEL array.

Acknowledgements – The research leading to these results has received funding from the ICT theme of the European Union Seventh Framework Programme (FP7/2007-2013) as part of the MiSPIA project (grant agreement No. 257646) and the project operated within the Foundation for Polish Science Team Programme co-financed by the European Regional Development Fund, Operational Program Innovative Economy 2007–2013.

References

- [1] GOMEZ-REINO C., PEREZ M.V., BAO C., *Gradient-Index Optics: Fundamentals and Applications*, Springer, Berlin, 2002.
- [2] KNITTEL J., SCHNIEDER L., BUSS G., MESSERSCHMIDT B., POSSNER T., *Endoscope-compatible confocal microscope using a gradient index-lens system*, *Optics Communications* **188**(5–6), 2001, pp. 267–273.
- [3] EITEL S., FANCEY S.J., GAUGGEL H.-P., GULDEN K.-H., BACHTOLD W., TAGHIZADEH M.R., *Highly uniform vertical-cavity surface-emitting lasers integrated with microlens arrays*, *IEEE Photonics Technology Letters* **12**(5), 2000, pp. 459–461.
- [4] OTOMA H., MURAKAMI A., KUWATA Y., UEKI N., MUKOYAMA N., KONDO T., SAKAMOTO A., OMORI S., NAKAYAMA H., NAKAMURA T., *Single-mode oxide-confined VCSEL for printers and sensors*, [In] *Proceedings of the 1st Electronics Systemintegration Technology Conference*, Vol. 1, 2006, pp. 80–85.
- [5] HUDELIST F., BUCZYNSKI R., WADDIE A.J., TAGHIZADEH M.R., *Design and fabrication of nanostructured gradient index microlenses*, *Optics Express* **17**(5), 2009, pp. 3255–3263.
- [6] HUDELIST F., NOWOSIELSKI J.M., BUCZYNSKI R., WADDIE A.J., TAGHIZADEH M.R., *Nanostructured elliptical gradient-index microlenses*, *Optics Letters* **35**(2), 2010, pp. 130–132.
- [7] NOWOSIELSKI J.M., BUCZYNSKI R., HUDELIST F., WADDIE A.J., TAGHIZADEH M.R., *Nanostructured GRIN microlenses for Gaussian beam focusing*, *Optics Communications* **283**(9), 2010, pp. 1938–1944.
- [8] BUCZYNSKI R., KUJAWA I., KASZTELANIC R., PYSZ D., BORZYCKI K., BERGHMANS F., THIENPONT H., STEPIEN R., *Supercontinuum generation in all-solid photonic crystal fiber with low index core*, *Laser Physics* **22**(4), 2012, pp. 784–790.

- [9] ZICKAR M., NOELL W., MARXER C., DE ROOIJ N., *MEMS compatible micro-GRIN lenses for fiber to chip coupling of light*, Optics Express **14**(10), 2006, pp. 4237–4249.
- [10] MILLER D.A.B., *Device requirements for optical interconnects to silicon chips*, Proceedings of the IEEE **97**(7), 2009, pp. 1166–1185.
- [11] SIHVOLA A., *Electromagnetic Mixing Formulas and Applications*, The Institution of Electrical Engineers, London, 1999.
- [12] HARTMANN A. K., RIEGER H., *Optimization Algorithms in Physics*, Wiley-VCH, Berlin, 2002.
- [13] TAFLOVE A., HAGNESS S.C., *Computational Electrodynamics: The Finite-Difference Time-Domain Method*, Artech House, Boston, 2000.
- [14] OSKOOI A.F., ROUNDY D., IBANESCU M., BERMEL P., JOANNOPOULOS J.D., JOHNSON S.G., *MEEP: A flexible free-software package for electromagnetic simulations by the FDTD method*, Computer Physics Communications **181**(3), 2010, pp. 687–702.
- [15] SERKLAND D.K., CHOQUETTE K.D., HADLEY G.R., GEIB K.M., ALLERMAN A.A., *Size dependence of small-aperture thin-oxide VCSELs*, Digest of the LEOS Summer Topical Meeting, San Diego, USA, 1999, pp. III15–III16.
- [16] SIEGMAN A.E., *Lasers*, University Science Books, Mill Valey, 1986.

*Received April 5, 2013
in revised form August 3, 2013*